Cell, Vol. 78, 1063–1072, September 23, 1994, Copyright © 1994 by Cell Press

Atomic Structure of the RuvC Resolvase: A Holliday Junction-Specific Endonuclease from E. coli

Mariko Ariyoshi,*† Dmitry G. Vassylyev,*† Hiroshi Iwasaki,‡ Haruki Nakamura,* Hideo Shinagawa,‡ and Kosuke Morikawa*
*Protein Engineering Research Institute
6–2–3 Furuedai
Suita
Osaka 565
Japan
‡Department of Molecular Microbiology
Research Institute for Microbial Diseases
Osaka University
3–1 Yamadaoka
Suita
Osaka 565
Japan

Summary

The crystal structure of the RuvC protein, a Holliday junction resolvase from E. coli, has been determined at 2.5 Å resolution. The enzyme forms a dimer of 19 kDa subunits related by a dyad axis. Together with results from extensive mutational analyses, the refined structure reveals that the catalytic center, comprising four acidic residues, lies at the bottom of a cleft that nicely fits a DNA duplex. The structural features of the dimer, with a 30 Å spacing between the two catalytic centers, provide a substantially defined image of the Holliday junction architecture. The folding topology in the vicinity of the catalytic site exhibits a striking similarity to that of RNAase H1 from E. coli.

Introduction

In all organisms, homologous recombination is a crucial process, not only for generating genetic diversity, but also for the repair of damaged chromosomes. The Holliday structure is a central intermediate of this cellular process, in which two homologous duplex DNA molecules are linked by a single-stranded crossover (Holliday, 1964). In Escherichia coli, recombinogenic DNA molecules with 3′ single-stranded regions are generated by the combined functions of DNA helicases and exonucleases during sexual conjugation or after DNA damages (Figure 1). The RecA protein, operating jointly with several other proteins, promotes homologous pairing and strand exchange between two homologous DNA molecules, which leads to the formation of a Holliday structure (for reviews, see West, 1992, 1994; Kowalczykowski et al., 1994). Heteroduplex regions in the Holliday structure are extended through branch migration of the junction promoted by the RuvA–RuvB protein complex (Iwasaki et al., 1992; Tsaneva et al., 1992) or by the RecG protein (Lloyd and Sharples, 1993). Reactions promoted by these proteins are thought to involve unwinding and rewinding of the duplex DNA at the junction and to be driven by their intrinsic ATP-dependent DNA helicase activity (Tsaneva et al., 1993). After these reactions, Holliday intermediates must be resolved to generate the recombinant molecules. This resolution process is catalyzed by the 19 kDa RuvC protein (172 amino acids), which cleaves the Holliday junction and produces unconnected DNA duplexes. Nicks, which are introduced at or near the crossover junction by RuvC, with both identical polarity and symmetry, are subsequently sealed by E. coli DNA ligase to generate two recombinant DNA duplexes (Dunderdale et al., 1991; Iwasaki et al., 1991).

The active form of RuvC in solution has been shown by gel filtration analysis to be dimeric (Iwasaki et al., 1991). The nicking activity requires divalent cations, such as Mg^{2+}. Mn^{2+} can substitute for Mg^{2+} with slightly lower efficiency, but Ca^{2+} and Zn^{2+} are poor substitutes (Bennett et al., 1993; Takahagi et al., 1994). Although divalent cations are essential for the RuvC endonuclease activity, in vitro studies, using small synthetic junctions as substrates, indicate that RuvC binds to a four-way junction efficiently without divalent cations. RuvC cleaves four-way junctions only when the junctions have sequence homology at the crossover. Studies using various synthetic junctions suggest that the binding and cleavage steps in Holliday junction resolution by RuvC are distinct, and that topological changes induced by spontaneous branch migration may play an important role in cleavage by RuvC (Takahagi et al., 1994). West and colleagues (Bennett et al., 1993) have shown that DNA distortion was induced by RuvC binding to the junction and that RuvC cleavage occurs at preferred sites, such as the 3′ side of a thymine residue. Although RuvC has the apparent sequence preference, it is obviously different in biological functions from resolvases involved in transposition or site-specific recombination. These enzymes act on reaction intermediates that include defined specific DNA sequences (Sherratt, 1989).

Endonucleases other than RuvC that can process Holliday junctions to produce unconnected DNA duplexes have been isolated or detected from several sources, including bacteriophages T4 and T7 (Mizuuchi et al., 1982; de Massy et al., 1984), yeast (Symington and Kolodner, 1985; West and Korner, 1985; Kleff et al., 1992), and mammals (Elborough and West, 1990; Hyde et al., 1994). Among them, T4 endonuclease VII and T7 endonuclease I have been extensively studied in vitro, and mechanisms for Holliday junction resolution have been proposed (Bhattacharyya et al., 1991). However, phage endonucleases are also involved in debranching DNA for packaging into the head particles and function as nucleases that degrade host DNA. The amino acid sequences of these phage endonucleases do not show any sequence similarity with that of RuvC (Sharples and Lloyd, 1991; Takahagi et al., 1991). In vitro, these endonucleases cleave synthetic four-way

†These two authors contributed equally to this work.

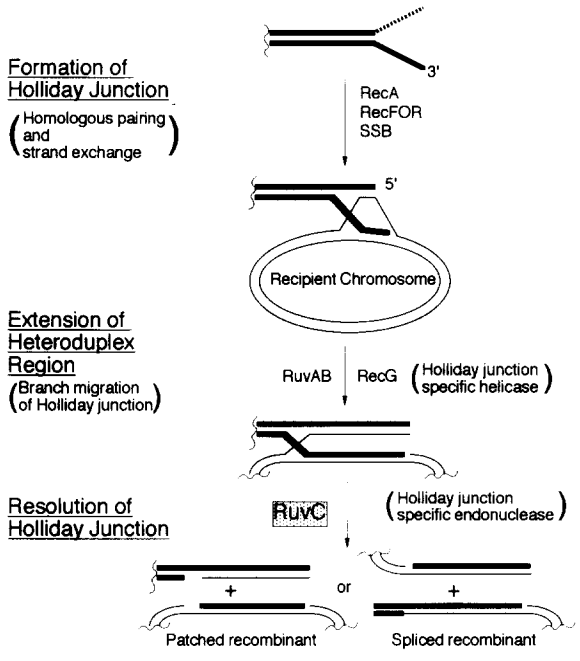

Figure 1. Formation and Resolution of a Holliday Junction in Homologous Recombination in E. coli

See text for explanation. Abbreviations are as follows: RecFOR, RecR, RecO, and RecR proteins; SSB, single-stranded binding protein.

junctions, irrespective of the presence of a homologous core DNA sequence. Therefore, unlike the phage endonucleases, RuvC appears to be devoted to the resolution of Holliday intermediates of homologous recombination.

Recently, it has been shown that RecA homologs exist in higher organisms, including yeast and human cells (Bishop et al., 1992; Shinohara et al., 1992, 1993; Morita et al., 1993). In particular, the Rad51 protein from Saccharomyces cerevisiae binds to DNA duplexes, forming helical nucleoprotein filaments that are remarkably similar to RecA filaments (Ogawa et al., 1993). These observations suggest that the essential cellular processes and mechanisms required for homologous recombination are well conserved from bacteria to human. A similar mechanism for resolving the Holliday junction is also likely to be shared between E. coli RuvC and its eukaryotic counterparts, since a RuvC-like activity has been detected in mammalian cells (Hyde et al., 1994).

To assist in a more precise understanding of the molecular basis for Holliday junction recognition as well as the catalytic mechanism, we have determined the three-dimensional (3D) structure of the RuvC protein at 2.5 Å resolution by X-ray crystallography. Together with results from mutational analysis of the *ruvC* gene carried out in parallel, the refined structure of the RuvC dimer allows the identification of the catalytic center and some possible interfaces with the Holliday junction.

Results and Discussion

Overall Structure

The crystal analyzed in the present study contains two dimeric molecules of the RuvC endonuclease in an asymmetric unit. The structure refined at 2.5 Å resolution includes 158 amino acids and roughly 50 ordered water molecules per subunit. The remaining segment (residues 159–172) at the carboxyl terminus is disordered in the crystal. This segment, which contains four Arg residues, appears to form a flexible and basic tail.

The molecule has a wedged shape with approximate dimensions 50 Å × 40 Å × 35 Å. The primary sequence with the secondary structure elements and a ribbon representation are shown in Figures 2A and 2B, respectively. The polypeptide chain is folded into a single domain that adopts an α plus β fold (Figure 2B). The molecule comprises five α helices (αA, αB, αC, αD, and αE) and a mixed β sheet with five strands (β1, β2, β3, β4, and β5). The β sheet includes three long antiparallel strands, β1, β2, and β3, at the amino terminus, and two short parallel strands, β4 and β5, between which the αB helix intervenes. The αA and αB helices are parallel and form hydrophobic interactions between them. The remaining three helices, αC, αD, and αE, form a helical core–like domain at the carboxyl terminus. The β sheet is thus sandwiched between the αA and αB helices on one side and the αC, αD, and αE helices on the other.

There is no substantial difference among the backbone structures of the four molecules in an asymmetric unit, except for the two loops containing residues 68–72 and 130–138, respectively. Root-mean-square displacements (rmsd) for superimposed Cα atoms between each pair of the four molecules are within the range of 0.73–1.01 Å.

The most remarkable feature of this structure is a large cleft (Figure 2B), with approximate dimensions of 20–25 Å wide and 20 Å deep, which is just sufficient to accommodate a double-stranded DNA. At the bottom of the cleft lies the amino terminal end of the αE helix. One side of the cleft is formed by a section of the sheet consisting of the three antiparallel β1, β2, and β3 strands, as well as the flexible loop (residues 68–72) that connects β4 to αB. The other side of the cleft is constructed partly by helices αC and αD and the loop following αD (residues 130–138). These walls are covered by eight basic residues pointing into the solvent, while four acidic residues are clustered at the bottom. The functional relevance of this cleft will be described in a later section.

Dimer Formation

The crystal structure reveals a dimeric form of RuvC (Figures 3A and 3B). The dimensions of the dimer are approximately 65 Å × 40 Å × 35 Å. The two protein subunits that form this dimer are related by a noncrystallographic 2-fold axis. The crystal contains two such dimers in the asymmetric unit. Figure 3A shows the superimposed Cα backbone structures of both dimers from the asymmetric unit. The rmsd value for the Cα atoms between these two dimers was calculated at 0.794 Å. This value, which is within the same range as the values for the individual monomer molecules, implies that the dimer conformation is not disrupted by the crystal packing effects.

Although the dimer interface involves both the αA and αB helices, the major contact for dimerization comes from the two αB helices arranged roughly parallel to the dyad axis

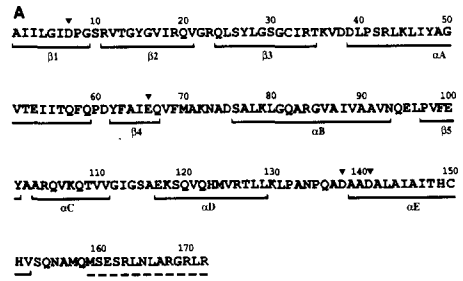

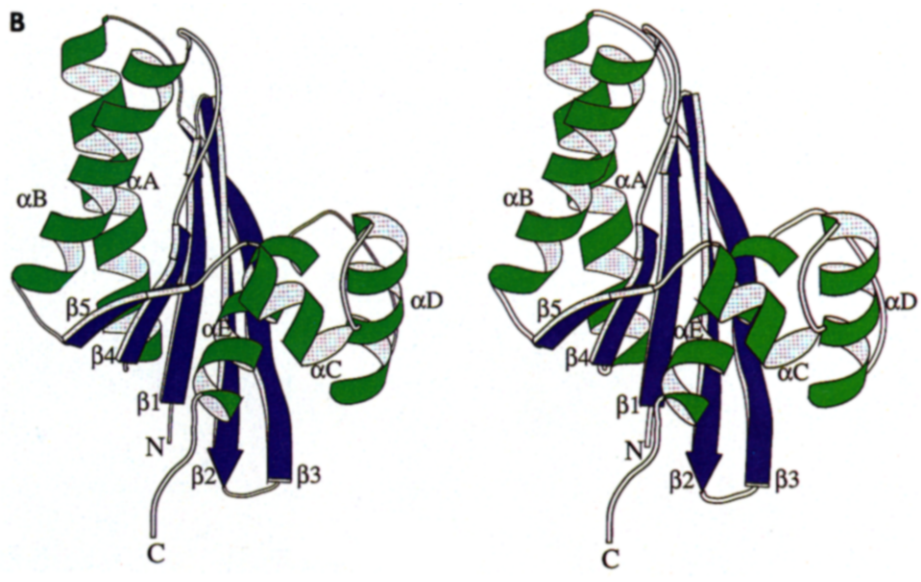

Figure 2. Primary Sequence of the RuvC Protein with the Secondary Structure, and Stereo Pair of Ribbon Model of the RuvC Monomer

(A) Primary sequence of the RuvC protein with the secondary structure elements. The amino acid sequence has been deduced from the base sequence of the *ruvC* gene (Takahagi et al., 1991). The secondary structure elements were defined according to the hydrogen bond criteria proposed by Kabsch and Sander (1983). Every tenth residue is numbered in the sequence. The four acidic residues involved in the endonuclease activity are marked with triangles. A dotted line indicates a disordered region in the crystal structure.

(B) Stereo pair of ribbon model of the RuvC monomer drawn with the program MOLSCRIPT (Kraulis, 1991). The β strands are colored in blue, and the α helices are in green. The secondary structure elements are labeled as in (A). The C-terminal disordered segment, which comprises fourteen residues (159–172), is excluded from the drawing. The DNA-binding cleft lies at the upper right side of the figure.

(Figure 3B). This contact involves both hydrophobic and polar interactions. For instance, a pair of hydrogen bonds is formed between the main chain carbonyl of Gly-81 in one subunit and the main chain imino group of Gln-82 in the other, respectively. Similarly, another pair of hydrogen bonds is formed between the side chains of Gln-82 and Arg-84 in the respective subunits. Nonpolar residues, such as Val-68, Leu-78, Leu-80, Val-86, and Val-89, contribute for intra- and intersubunit interactions in the dimer interface. In addition, an intersubunit hydrophobic contact, between Leu-44 in the αA helix and Ile-88 in the αB helix, partly stabilizes the dimer.

These features of the dimeric interface are consistent with various results from mutational analyses. For instance, *ruvC* mutant genes altering Leu-44, Val-68, Leu-78, Leu-80, or Val-86 (L44P, V68D, L78P/Q, L80P/Q and V86E), which are directly involved in dimerization, failed to complement the UV sensitivity of a *ruvC* strain (H. I., K. Ichiyanagi, T. Hishida, and H. S., unpublished data).

Active Site

In parallel with the crystallographic study, extensive mutational analyses were carried out to identify both the catalytic center and the DNA interface. Two single point mutations of each of four acidic residues, Asp-7, Glu-66, Asp-138, and Asp-141 (D7N/E, E66Q/D, D138N/E, or D141N/E), all caused the loss of DNA repair activity in vivo. The RuvC proteins purified from these mutants were defective in cleaving synthetic Holliday junctions, while they retained the normal binding activity to the junctions (A. Saito, H. I., and H. S., unpublished data). Similar substitutions for other acidic residues in RuvC did not affect the DNA repair function of the protein in vivo. The RuvC endonuclease requires divalent cations, such as Mg^{2+}, for junction cleavage but not for binding (Bennett et al., 1993; Takahagi et al., 1994). Recent crystallographic studies of various divalent metal ion–requiring nucleases, such as E. coli RNAase H1 (Katayanagi et al., 1992, 1993) and the 3′–5′ exonuclease domain of E. coli DNA polymerase I (Beese and Steitz, 1991), have demonstrated that their catalytic centers involve three or four acidic residues, at least some of which are coordinated to a metal cation (Beese and Steitz, 1991; Katayanagi et al., 1993). These findings being taken into consideration, the four acidic residues identified by mutational analyses are likely to constitute the catalytic center for the RuvC endonuclease.

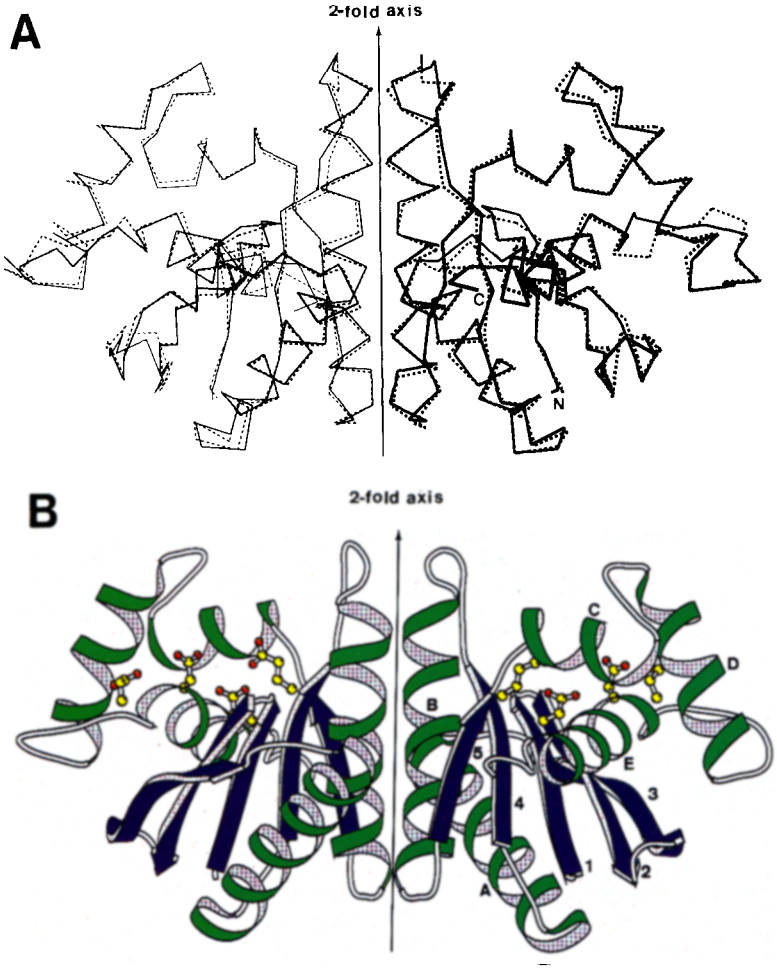

Figure 3. Dimeric Structure of RuvC

(A) Cα superposition of two dimers forming the asymmetric unit. These are shown as solid and dotted lines. The symmetry relationship between the respective dimers is shown in thick and thin lines. Both αB helices run parallel to the 2-fold axis.

(B) Ribbon drawing (Kraulis, 1991) of the dimer viewed as in (A). The β strands are numbered, and the α helices are lettered as in Figure 2A. The catalytic residues Asp-7, Glu-66, Asp-138, and Asp-141 are shown as ball-and-stick models in each subunit.

In agreement with these results, the four acidic residues, which are dispersed in the primary structure, are concentrated at the bottom of the putative DNA-binding cleft within the monomeric RuvC structure (Figure 3B). Except for Asp-138, the conformations of the three residues Asp-7, Glu-66, and Asp-141 are superimposed well among the four molecules in an asymmetric unit. Furthermore, the walls of the cleft contain eight basic residues whose side chains are mostly directed toward the center of the cleft. They are likely to interact with phosphate backbones of a Holliday junction during hydrolysis. We have soaked crystals in Mn^{2+} solutions to identify the bound metal on a difference Fourier map. The map, calculated from a crystal soaked in 5 mM $MnCl_2$ solution, exhibited a significant peak (above 3σ) at distances of 2.5 Å and 3.5 Å from the side chain $O_{\varepsilon 1}$ of Asp-7 and the side chain $O_{\varepsilon 2}$ of Asp-141, respectively, within only one molecule in the asymmetric unit. A Mn^{2+} concentration exceeding 5 mM caused cracks too serious for data collection to be accomplished. Molecular arrangements within the crystal imply that the acidic catalytic centers of four molecules in the asymmetric unit are at least partly blocked by the disordered and basic carboxyl termini belonging to other molecules. This may account for the crystal disruption induced by soaking of Mn^{2+}.

In the active dimer, the two catalytic centers are approximately 30 Å apart from each other, and the dimeric pair of the prominent loop (residues 68–72) and the amino end of the following αB helix form a partitioning wall between the two clefts.

Interaction with the Holliday Junction

Examination of charge distribution on the RuvC molecular surface should allow the identification of a possible interface with the Holliday junction, since DNA phosphate backbones are assumed to interact with basic residues of the protein. A display of the electrostatic potentials on the dimeric solvent-accessible surface (Nakamura and Nishida, 1987) reveals the biased localization of acidic and basic residues, which are shown in red and blue, respectively (Figure 4). Notable charge distributions are observed in the large cleft where each monomer is assumed to accommodate a DNA duplex. The clear contrast of red and blue regions identifies the negative charges of Asp-7, Glu-66, Asp-138, and Asp-141, which constitute the catalytic center, at the bottom of the cleft, while the walls of the cleft are covered by positive charges contributed by Arg-11, Arg-34, Lys-36, Lys-72, Lys-79, Arg-104, Lys-107, and Lys-118. As described in the previous section, the mutational analyses support the proposal that the cluster of the four

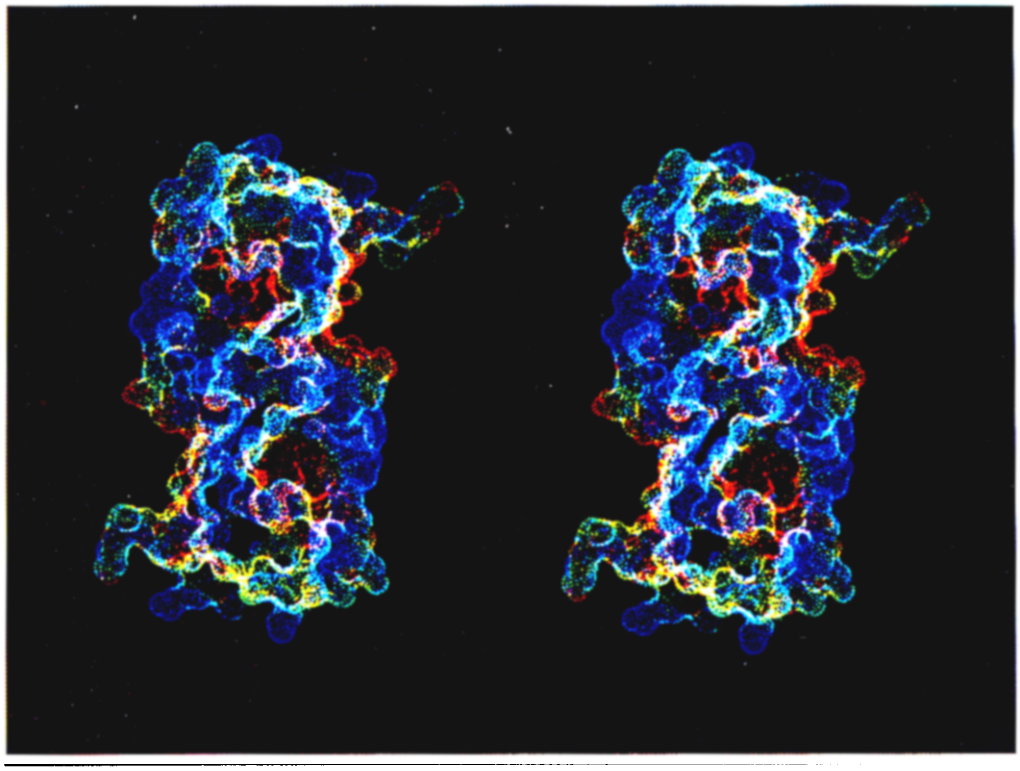

Figure 4. Color Display of the Electrostatic Potential on the Solvent-Accessible Surface of the RuvC Dimer

The dimeric molecules rotated by 90° about the internal 2-fold axis in Figure 3 are seen parallel to the same axis from the top. Red indicates electrostatic potential values below −0.05 V, blue above +0.05 V, and green between +0.05 and −0.05 V. The calculation was performed at pH 7.0.

acidic residues participates in the junction cleavage. Additional analyses show that RuvC loses its DNA repair activity by the replacements of Arg-104 by His (R104H) and Lys-118 by Arg (K118R) (H. I., K. Ichiyanagi, T. Hishida, and H. S., unpublished data). Together with these results, the structure suggests that at least two residues, Arg-104 and Lys-118, are involved in the junction binding.

In an attempt to build a tentative model of the complex, docking studies have been implemented using molecular graphics, with the stacked X structure (von Kitzing et al., 1990; Clegg et al., 1992) as the initial substrate model. This junction structure possesses a 2-fold axis, which passes through an exchange point of the DNA strands. It is reasonable to assume that this 2-fold axis of the junction structure coincides with the internal dyad axis of the RuvC dimer. However, we were unable to fit this structure simultaneously into both DNA binding clefts that are 30 Å apart from each other in the dimer. In particular, serious steric hindrance caused by the prominent wall between the two clefts made this model unrealistic. It is also clear that the square planar structure (von Kitzing et al., 1990), presumed to exist in the absence of metal cations, does not fit into the RuvC dimer. Thus, we adopted a different strategy for model building. First, we fitted a homologous B-form DNA duplex into each cleft in the dimer, so that they were related by a noncrystallographic 2-fold axis. Next, at the best-fit position to the two clefts, these two DNA duplexes were covalently linked by connecting nucleotides and energetically optimized by the use of the PRESTO program package (Morikami et al., 1992). This procedure allowed the construction of a reasonable model for the Holliday junction (Figure 5A), assuming that both junction cleavages take place simultaneously. This model, which consists of two antiparallel quasicontinuous DNA duplexes, is entirely similar to the stacked X structure (von Kitzing et al., 1990). However, the two models of the Holliday junction are different in the local structure around the exchange point of DNA strands; our model has longer extended linkers with at least two nucleotides. In this model of the RuvC–junction complex, the interface of RuvC covers a DNA duplex of 9 bp that is inclined by about 80° to the dyad axis of a dimer. The residue of Phe-69, which lies in the protruding loop preceding the αB helix, makes a stacking interaction with a nucleotide base located close to a junction point. Indeed, the mutation from Phe-69 to Leu causes loss of DNA repair activity in vivo (H. I., K. Ichiyanagi, T. Hishida, and H. S., unpublished data). The stacked X structure may exist as a protein-free structure. The productive interaction between RuvC and the junction DNA may induce the conformational change of the junction to our model, and then the junction of cleavage would take place. The requirement of homologous core sequence in the junctions for RuvC-mediated cleavage (Bennett et al., 1993; Takahagi et al., 1994) may reflect the facilitation of such a conformational change induced by spontaneous branch migration.

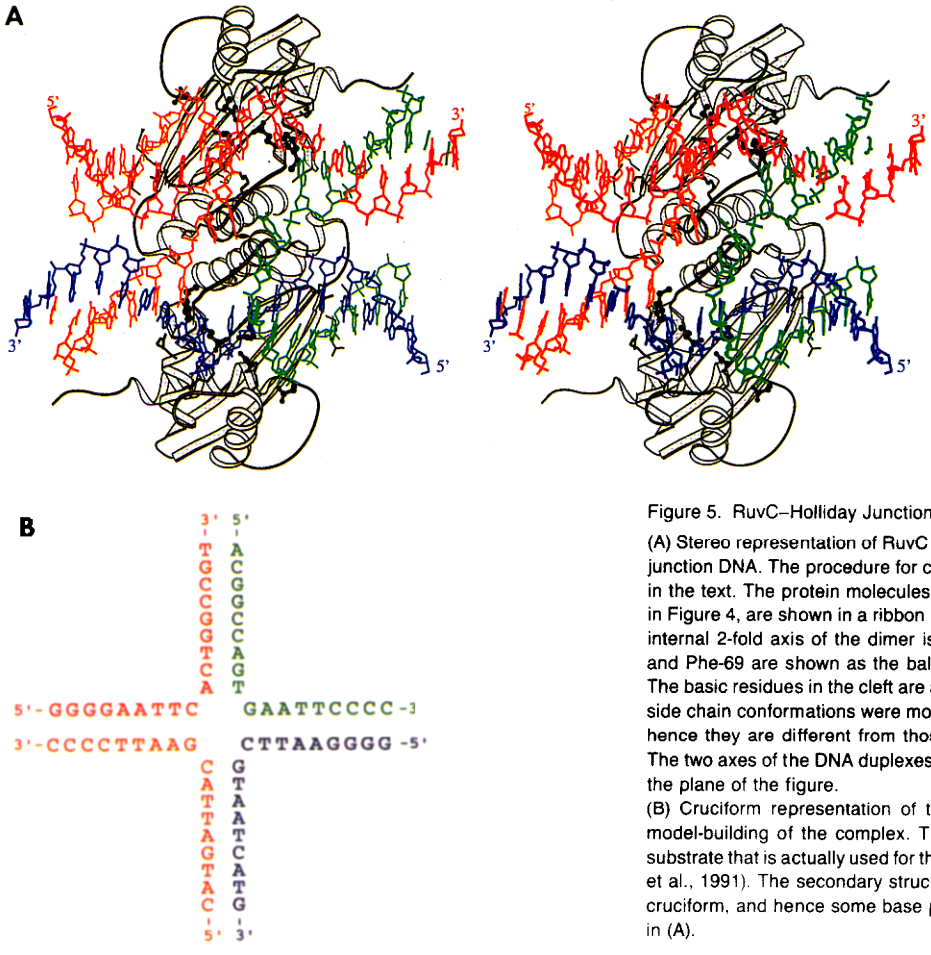

Figure 5. RuvC–Holliday Junction Complex

(A) Stereo representation of RuvC dimer in complex with the Holliday junction DNA. The procedure for constructing the model is described in the text. The protein molecules, with the same orientation as that in Figure 4, are shown in a ribbon representation (Kraulis, 1991). The internal 2-fold axis of the dimer is indicated. The catalytic residues and Phe-69 are shown as the ball-and-stick model in each subunit. The basic residues in the cleft are also indicated by solid lines. These side chain conformations were modified by energy minimization, and hence they are different from those in the refined crystal structure. The two axes of the DNA duplexes separate by 10° above and below the plane of the figure.

(B) Cruciform representation of the DNA sequences used for the model-building of the complex. The sequences are derived from a substrate that is actually used for the cleavage assay of RuvC (Iwasaki et al., 1991). The secondary structure is displayed in a conventional cruciform, and hence some base pairs are not consistent with those in (A).

Thus, the docking examination based on the substrate-free crystal structure has allowed the construction of a model that is consistent with various aspects of the RuvC–substrate DNA interaction. However, we are aware that the validity of the model has to be critically examined by various physicochemical experiments, including direct determination of the enzyme–junction complex.

Structural Similarity to RNAase H1

The structure of the RuvC protein shows a striking topological resemblance to that of E. coli RNAase H1 (Katayanagi et al., 1990, 1992; Yang et al., 1990), despite the lack of any sequence similarity (Figure 6). Even visual inspection of their architectures obviously indicates that the five-stranded β sheet and the αA helix connecting the β3 and β4 strands are arranged identically in both structures. Comparison of the common structural motif in RuvC and RNAase H1 (β1, β2, β3, β4, and αA) superimposes 35 Cα atoms with an rmsd value of 2.1 Å.

RNAase H1 is an endonuclease that specifically degrades only the RNA strand of a DNA–RNA hybrid duplex to produce 5′-phosphate groups at the hydrolysis site. This enzyme requires a divalent metal ion such as Mg^{2+} or Mn^{2+} for the catalytic activity. The RuvC endonuclease cleaves the P-O3′ bond of a DNA backbone to produce a 5′-phosphate group and also requires a similar divalent metal ion. However, it has been shown that RNAase H1 acts in a monomeric state (Kanaya et al., 1989), whereas the active form of the RuvC protein is a dimer (Iwasaki et al., 1991).

Thus, these two endonucleases have similar catalytic reactions, even though their target molecules for cleavage and functional subunit structures differ. In fact, the remarkable resemblance emerges from the comparison of their catalytic centers. As described in the previous section, the catalytic center of the RuvC endonuclease consists of four acid residues, Asp-7, Glu-66, Asp-138, and Asp-141. Similarly, the catalytic center of RNAase H1 comprises four invariant acidic residues, Asp-10, Glu-48, Asp-70, and Asp-134, and three of them, Asp-10, Asp-70, and Glu-48, are known to be essential for the activity (Katayanagi et al., 1990, 1993; Yang et al., 1990). It is noteworthy that three of the residues, Asp-7, Glu-66, and Asp-141, are well superimposed on the three essential residues Asp-10, Glu-48, and Asp-70 in RNAase H1, with an rmsd value of 2.2 Å for the atomic positions, including the side chain atoms.

As described before, the two αB helices provide the interface for dimerization. Consistent with this functional difference, RNAase H1 lacks the corresponding helix, but it contains an insertion of three helices, αB, αC, and αD, in place of the αB helix in the RuvC molecule. These three helices in RNAase HI provide a particular interface with

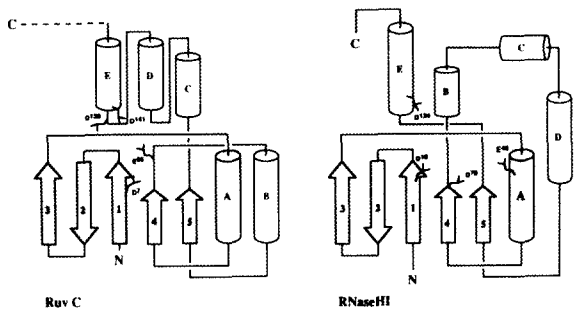

Figure 6. Topological Diagrams of RuvC and RNAase H1

The β strands are represented as numbered broad arrows, and the α helices are lettered cylinders. Common secondary structure elements between RuvC and RNAase H1 are shadowed. The catalytic residues of RuvC (Asp-7, Glu-66, Asp-138, and Asp-141) are shown in solid lines. The corresponding residues of RNAase H1 (Asp-10, Glu-48, Asp-70, and Asp-134) are also shown.

a DNA–RNA hybrid. Furthermore, the αE helix, flanking the β sheet in RNAase H1, is replaced by the helical core consisting of the three helices αC, αD, and αE in the RuvC protein. It is likely that these two enzymes diverged from a common ancestor bearing a catalytic field for the divalent metal ion–dependent nuclease activity. However, an alternative explanation also may be possible, namely, that the two enzymes have converged from different ancestors into nucleases with similar catalytic fields, since there is no significant similarity between their primary structures nor between the nucleotide sequences of the *ruvC* and *rnhA* genes.

To detect other proteins relevant to the RuvC endonuclease, sequence analyses and searches by 3D–1D compatibility assessment (Nishikawa and Matsuo, 1993) were performed. However, in terms of both the primary and tertiary structures, no significant similarity was found with any other protein, including T4 endonuclease VII and T7 endonuclease I.

Experimental Procedures

Crystallization, Data Collection, and Structural Analysis

The RuvC protein was crystallized as previously reported (Ariyoshi et al., 1994). Crystals belong to the monoclinic space group $P2_1$, with unit cell dimensions a = 72.8 Å, b = 139.6 Å, c = 32.4 Å, and β = 93.0°, and contain four molecules per asymmetric unit. However, a low resolution diffraction pattern to about 5 Å exhibits a pseudosymmetry of $P22_12$.

A medium resolution intensity data set to 3.0 Å was collected from native crystals (Table 1) by using an automated imaging plate diffractometer DIP100 (Mac Science) with CuKα radiation, generated by a rotating anode M18X (Mac Science) operated at 45 kV and 90 mA. The diffraction images were processed with the program ELMS (Tanaka et al., 1990) and merged using the program PROTEIN (Steigemann, 1974). A higher resolution native data set was collected to 2.5 Å using a Weissenberg-type imaging diffractometer (Sakabe, 1991) installed on beam line BL6A of the Synchrotron Radiation Source at the Photon Factory, Tsukuba. The wavelength was set to 1.0 Å. Imaging data

Table 1. Statistics of Crystallographic Data

Data sets		Native[a]	Native	HGCL1[a,b]	HGCL2[a,c]	HGCL3[d]	PTCL[e]	
Wave length (Å)		1.00	1,54	1.54	0.92	1.00	1.54	
Resolution limit (Å)		2.5	3.0	3.0	3.0	3.0	3.0	
Number of reflections		17,615	10,989	9,670	11,239	11,166	6,974	
(Completeness)		(0.810)	(0.900)	(0.793)	(0.935)	(0.928)	(0.660)	
R_{merge}		0.060	0.054	0.10	0.075	0.060	0.064	
R_{iso}		–	–	0.16	0.16	0.16	0.20	
Number of heavy atom sites		–	–	14	15	15	14	
Phasing power		–	–	1.43	1.99	2.03	0.72	
R_{Cullis}		–	–	0.73	0.68	0.68	0.73	
Mean Figure of Merit								
Resolution (Å)	15.63	9.76	7.10	5.57	4.59	3.90	3.39	3.00	
Acentric	0.795	0.846	0.840	0.810	0.757	0.708	0.651	0.600	0.689 total
Centric	0.730	0.979	0.919	0.860	0.920	0.931	0.898	0.851	0.897 total
Refinement								
Resolution			6.0–2.5 Å					
R factor			0.157					
Number of reflections			15,545					
Number of protein atoms			4,768					
Number of water atoms			198					
rms bond length[f]			0.013 Å					
rms bond angle[f]			0.039 Å					

R_{merge}, $\Sigma\Sigma \mid I_{h,j} - \langle I_h \rangle \mid / \Sigma\Sigma \langle I_h \rangle$; R_{Cullis}, $\Sigma \mid F_{PH} \pm F_P \mid - F_{H(calc)} \mid / \Sigma \mid F_{PH} - F_P \mid$ (for centric reflections); R_{iso}, $\Sigma \parallel F_{PH} \mid - \mid F_P \parallel / \Sigma \mid F_P \mid$. Where $I_{h,j}$ = measured diffraction intensity, $\langle I_h \rangle$ = mean value of all intensity measurements of (h,k,l) reflection; F_{PH} = structure amplitude of a derivative; F_P = structure amplitude of the native crystal; $F_{H(CALC)}$ = the calculated contribution of the heavy atoms. Phasing power is the ratio of the root mean square (rms) heavy atom scattering factor amplitude to the rms lack of closure error.

[a] Intensity data collected using a synchrotron source.

[b] HGCL1: 2 mM $HgCl_2$ for 18 hr (pH 8.0).

[c] HGCL2: 5 mM $HgCl_2$ for 7 hr (pH 8.0).

[d] HGCL3: 5 mM $HgCl_2$ for 3 hr (pH 8.0).

[e] PTCL: 2 mM K_2PtCl_4 for 20 hr (pH 8.0).

[f] rms deviation from ideality.

were processed using the program WEIS (Higashi, 1989). The final, complete model was refined with this data set.

Isomorphous heavy atom derivatives were prepared at room temperature by soaking crystals in various heavy atom solutions. A suitable condition for the Pt derivative was an exposure to a 2 mM K_2PtCl_4 solution for 20 hr. Three $HgCl_2$ derivatives with different occupancies were prepared under various conditions for heavy atom concentrations or soaking times within the ranges of 2–5 mM $HgCl_2$ and 5–18 hr, respectively. The program PROTEIN was used for local scaling of the derivative data sets to the native data. Initially, two derivative data sets of K_2PtCl_4 and $HgCl_2$ (PTCL and HGCL1) were collected to 3.0 Å using an imaging plate diffractometer. The initial multiple isomorphous replacement (MIR) analysis was carried out with these derivative data and the medium resolution native data. Three major $HgCl_2$ sites were identified using the automatic Patterson search program HASSP (Terwilliger et al., 1987). Four major K_2PtCl_4 sites were revealed by difference Fourier syntheses and by inspection of difference Patterson maps. The heavy atom positions were confirmed using the direct-method program MULTAN (Main et al., 1980). This process was carried out according to essentially the same procedure as reported by Navia and Sigler (1974) and Wilson (1978). Heavy atom positions and occupancies were refined using the program MLPHARE from CCP4 (SERC Collaborative Computing Project Number 4, a Suit of Programs for Protein Crystallography [Daresbury Laboratory, Warrington, England]).

The initial phases were calculated on the basis of these derivatives, including anomalous data, but neither clear molecular boundaries nor secondary structure elements were discernible in this MIR map. Additional data sets from two different $HgCl_2$ derivatives (HGCL2 and HGCL3) were then collected at wavelengths of 1.00 Å and 0.92 Å, respectively, using the Synchrotron Radiation Source at the Photon Factory. The difference Fourier maps, calculated from phases refined with the additional $HgCl_2$ derivatives, revealed new heavy atom sites. Then, MIR phases were calculated from all four derivatives at 3.0 Å, using both isomorphous and anomalous data, to produce a new MIR map. This MIR map was subjected to solvent flattening (Wang, 1985) by use of programs from the CCP4 suit, as described by Leslie (1987). Heavy atom parameters were refined against the solvent-flattened phases, and MIR phases were recalculated on the basis of these refined heavy atom parameters (Cura et al., 1992; Rould et al., 1992). The map calculated from these improved phases allowed us to discern some α helices and β strands, but it was still too poor to achieve an unambiguous chain tracing. The molecular averaging technique in real space (Bricogne, 1976) was then applied for further improvement of the phases. First, the noncrystallographic symmetry was examined between two dimeric molecules in an asymmetric unit, from three pairs of the refined heavy atom positions. Their correlation coefficients were evaluated to be about 0.7. Only one pair of heavy atoms was found inside the dimer. A real-space rotation function search, using the program PROTEIN, was then applied to find the orientation between the molecules within the dimer. About 2000 peaks were selected from the solvent-flattened electron density map inside a sphere with a radius of 10 Å, which is completely included in one of the molecules. These peaks were then rotated for all possible angles in polar angular space, with steps of 5° around the middle point, taken as the origin, between two equivalent heavy atom positions, and in each step, correlation function between the rotated and unrotated densities was calculated. The rotation function showed one strong peak, corresponding to the correct orientation. This orientation was then refined by the GAP program (D. I. Stuart and J. Grimes, unpublished data). To define a molecular envelope for averaging, dummy atoms were placed as spheres with radii of 4.0 Å on the solvent-flattened map for one molecule in an asymmetric unit. The set of dummy atoms for one molecule was calculated automatically by the program MOLENV (D. G. V., unpublished data). The molecular envelope was automatically calculated by the use of the program GAP. The envelopes of the other three molecules were generated by a noncrystallographic symmetry operation. The averaging was iterated 25 cycles at 3.0 Å by use of the program GAP. The molecular envelopes were revised by using the new averaged map. A further 25 cycles of averaging achieved a convergence, to provide a final correlation value of 0.85. After confirming the obvious improvement of the map, the phases were extended from 3.0 Å to 2.5 Å in a continuous series of 1/500 Å with iterative 300 cycles of molecular averaging. The correlation coefficients increased to 0.88, and the electron density map thus obtained allowed an unambiguous chain tracing.

Model Building and Crystallographic Refinement

For construction of the initial model, the Cα atoms belonging to one molecule in an asymmetric unit were fitted into the 3 Å resolution averaged electron densities. Then, peptide backbones derived from a data base of refined structures were created around the Cα atoms to produce a polyalanine model of the RuvC protein. These procedures were carried out by the use of computer graphics program O (Jones et al., 1991). Next, the side chains of the respective residues were replaced by what fit to electron densities. Three models for the remainders in the asymmetric unit were generated by application of the noncrystallographic symmetry operation. Crystallographic refinement was carried out by energy minimization and simulated annealing with molecular dynamics using the X-PLOR package (Brünger, 1993). This process dropped the R factor from 43.0% to 19.5%. Six rounds of refinement and manual model rebuilding extended the resolution from 3.0 Å to 2.5 Å, resulting in an R factor of 18.0%. Subsequently, by use of the program PROLSQ (Hendrickson and Konnert, 1980), two rounds of restrained least square refinement were carried out to provide the present model. The average B-factors for all the main chain atoms are 25.5 $Å^2$, 26.3 $Å^2$, 27.8 $Å^2$, and 26.4 $Å^2$ for the four molecules, respectively.

Acknowledgments

We thank A. Saito, K. Ichiyanagi, and T. Hishida for providing data of *ruvC* mutants before publication, and K. Kamada and N. Isomura for their help in RuvC purification. We appreciate Drs. M. Swindells and A. Murzin for their useful discussions and comments. Drs. K. Nishikawa and Y. Matsuo are acknowledged for sequence analyses and the 3D–1D compatibility assessment. This work was supported in part by Grants in Aid for Scientific Research from the Ministry of Education, Science, and Culture of Japan to H. I. and H. S.

Received July 25, 1994; revised August 16, 1994.

References

Ariyoshi, M., Vassylyev, D. G., Fujishima, A., Iwasaki, H., Shinagawa, H., and Morikawa, K. (1994). Preliminary crystallographic study of *Escherichia coli* RuvC protein: an endonuclease specific for Holliday junctions. J. Mol. Biol. *241*, 281–282.

Beese, L. S., and Steitz, T. A. (1991). Structural basis for the 3′–5′ exonuclease activity of *Escherichia coli* DNA polymerase I: a two metal ion mechanism. EMBO J. *10*, 25–33.

Bennett, R. J., Dunderdale, H. J., and West, S. C. (1993). Resolution of Holliday junctions by RuvC resolvase: cleavage specificity and DNA distortion. Cell *74*, 1021–1031.

Bhattacharyya, A., Murchie, A. I. H., von Kitzing, E., Diekmann, S., Kemper, B., and Lilley, D. M. J. (1991). Model for the interaction of DNA junctions and resolving enzymes. J. Mol. Biol. *221*, 1191–1207.

Bishop, D. K., Park, D., Xu, L., and Kleckner, N. (1992). *DMC1*: a meiosis-specific yeast homolog of E. coli *recA* required for recombination, synaptonemal complex formation, and cell cycle progression. Cell *69*, 439–456.

Bricogne, G. (1976). Methods and programs for direct-space exploitation of geometric redundancies. Acta Cryst. (A) *32*, 832–847.

Brünger, A. T. (1993). X-PLOR Version 3.1 (New Haven: Yale University Press).

Clegg, R. M., Murchie, A. I. H., Zechel, A., Carlberg, C., Diekmann, S., and Lilley, D. M. J. (1992). Fluorescence resonance energy transfer analysis of the structure of the four-way DNA junction. Biochemistry *31*, 4846–4856.

Cura, V., Khrishnaswamy, S., and Podjarny, A. D. (1992). Heavy-atom refinement against solvent-flattened phases. Acta Cryst. (A) *48*, 756–764.

de Massy, B., Studier, F. W., Dorgai, L., Appelbaum, E., and Weisberg, R. A. (1984). Enzymes and sites of genetic recombination: studies

with gene-3 endonuclease of phage T7 and with site-affinity mutants of phage λ. Cold Spring Harbor Symp. Quant. Biol. *49*, 715–726.

Dunderdale, H. J., Benson, F. E., Parsons, C. A., Sharples, G. J., Lloyd, R. G., and West, S. C. (1991). Formation and resolution of recombination intermediates by *E. coli* RecA and RuvC proteins. Nature *354*, 506–510.

Elborough, K. M., and West, S. C. (1990). Resolution of synthetic Holliday junctions in DNA by an endonuclease activity from calf thymus. EMBO J. *9*, 2931–2936.

Hendrickson, W. A., and Konnert, J. H. (1980). Incorporation of stereochemical information into crystallographic refinement. In Computing in Crystallography, R. Diamond, S. Ramaseshan, and K. Venkatesan, eds. (Bangalore, India: Indian Academy of Science, International Union of Crystallography), pp. 13.01–13.23.

Higashi, T. (1989). The processing of diffraction data taken on a screenless Weissenberg camera for macromolecular crystallography. J. Appl. Cryst. *22*, 9–18.

Holliday, R. (1964). A mechanism for gene conversion in fungi. Genet. Res. *5*, 282–304.

Hyde, H., Davies, A. A., Benson, F. E., and West, S. C. (1994). Resolution of recombination intermediates by a mammalian activity functionally analogous to *Escherichia coli* RuvC resolvase. J. Biol. Chem. *269*, 5202–5209.

Iwasaki, H., Takahagi, M., Shiba, T., Nakata, A., and Shinagawa, H. (1991). *Escherichia coli* RuvC protein is an endonuclease that resolves the Holliday structure. EMBO J. *10*, 4381–4389.

Iwasaki, H., Takahagi, M., Nakata, A., and Shinagawa, H. (1992). *Escherichia coli* RuvA and RuvB proteins specifically interact with Holliday junctions and promote branch migration. Genes Dev. *6*, 2214–2220.

Jones, T. A., Zou, J. Y., Cowan, S. W., and Kjeldgaard, M. (1991). Improved methods for building protein models in electron density maps and location of errors in these models. Acta. Cryst. (A) *47*, 110–119.

Kabsch, W., and Sander, C. (1983). Dictionary of protein secondary structure: pattern recognition of hydrogen-bonded and geometrical features. Biopolymers *22*, 2577–2637.

Kanaya, S., Kohara, A., Miyagawa, M., Matsuzaki, T., Morikawa, K., and Ikehara, M. (1989). Overproduction and preliminary crystallographic study of ribonuclease H from *Escherichia coli*. J. Biol. Chem. *264*, 11546–11549.

Katayanagi, K., Miyagawa, M., Matsushima, M., Ishikawa, M., Kanaya, S., Ikehara, M., Matsuzaki, M., and Morikawa, K. (1990). Three-dimensional structure of ribonuclease H from *E. coli*. Nature *347*, 306–309.

Katayanagi, K., Miyagawa, M., Matsushima, M., Ishikawa, M., Nakamura, H., Ikehara, M., Matsuzaki, T., and Morikawa, K. (1992). Structural details of ribonuclease H from *Escherichia coli* as refined to an atomic resolution. J. Mol. Biol. *223*, 1029–1052.

Katayanagi, K., Okumura, M., and Morikawa, K. (1993). Crystal structure of *Escherchia coli* RNaseHI in complex with Mg^{2+} at 2.8 Å resolution: proof for a single Mg^{2+}-binding site. Proteins *17*, 337–346.

Kleff, S., Kemper, B., and Sternglanz, R. (1992). Identification and characterization of yeast mutants and the gene for a cruciform cutting endonuclease. EMBO J. *11*, 699–704.

Kowalczykowski, S. C., Dixon, D. A., Eggleston, A. K., Lauder, S. D., and Rehrauer, W. M. (1994). Biochemistry of homologous recombination in *Escherichia coli*. Microbiol. Rev. *58*, 401–465.

Kraulis, P. J. (1991). MOLSCRIPT: a program to produce both detailed and schematic plots of protein structures. J. Appl. Cryst. *24*, 946–950.

Leslie, A. G. W. (1987). A reciprocal-space method for calculating a molecular envelope using the algorithm of B. C. Wang. Acta Cryst. (A) *43*, 134–136.

Lloyd, R. G., and Sharples, G. J. (1993). Dissociation of synthetic Holliday junctions by *E. coli* RecG protein. EMBO J. *12*, 17–22.

Main, P., Fiske, S. J., Germain, G., Hull, S. E., Dsclercq, J. P., Lessinfer, L., and Woolfson, M. M. (1980). MULTAN 80: A System of Computer Programs for the Automatic Solution of Crystal Structures from X-Ray Diffraction Data (York, England: Universities of York, England, and Louvain, Belgium).

Mizuuchi, K., Kemper, B., Hays, J., and Weisberg, R. A. (1982). T4 endonuclease VII cleaves Holliday structures. Cell *29*, 357–365.

Morikami, K., Nakai, T., Kidera, A., Saito, M., and Nakamura, H. (1992). PREST (Protein Engineering Simulator): a vectorized molecular mechanics program for biopolymers. Computers Chem. *16*, 243–248.

Morita, T., Yoshimura, Y., Yamamoto, A., Murata, K., Mori, M., Yamamoto, H., and Matsushiro, A. (1993). A mouse homologue of *Escherichia coli recA* and *Saccharomyces cervisiae RAD51* genes. Proc. Natl. Acad. Sci. USA *90*, 6577–6580.

Nakamura, H., and Nishida, S. (1987). Numerical calculations of electrostatic potentials of protein-solvent systems by the self consistent boundary method. J. Phys. Soc. Japan *56*, 1609–1622.

Navia, M. A., and Sigler, P. B. (1974). The application of direct methods to the analysis of heavy-atom derivatives. Acta Cryst. (A) *30*, 706–712.

Nishikawa, K., and Matsuo, Y. (1993). Development of pseudoenergy potentials for assessing protein 3D–1D compatibility and detecting weak homologies. Protein Eng. *6*, 811–820.

Ogawa, T., Yu, X., Shinohara, A., and Egelman, E. H. (1993). Similarity of the yeast Rad51 filament to the bacterial RecA filament. Science *259*, 1896–1899.

Rould, M. A., Perona, J. J., and Steitz, T. A. (1992). Improving multiple isomorphous replacement phasing by heavy-atom refinement using solvent flattened phases. Acta Cryst. (A) *48*, 751–756.

Sakabe, N. (1991). X-ray diffraction data collection system for modern protein crystallography with a Weissenberg camera and an imaging plate using synchrotron radiation. Nucl. Instrum. Meth. Phys. Res. Sect. A *303*, 448–463.

Sharples, G. J., and Lloyd, R. (1991). Resolution of Holliday junctions in *Escherichia coli*: identification of the *ruv*C gene product as a 19-kilodalton protein. J. Bacteriol. *173*, 7711–7715.

Sherratt, D. (1989). Tn3 and related transposable elements: site-specific recombination and transposition. In Mobile DNA, D. E. Berg and M. M. Howe, eds. (Washington, D. C.: American Society for Microbiology), pp. 163–184.

Shinohara, A., Ogawa, H., and Ogawa, T. (1992). Rad51 protein involved in repair and recombination in S. cerevisiae is a RecA-like protein. Cell *69*, 457–470.

Shinohara, A., Ogawa, H., Matsuda, Y., Ushio, N., Ikeo, K., and Ogawa, T. (1993). Cloning of human, mouse, and fission yeast recombination genes homologous to *Rad51* and *recA*. Nature Genet. *4*, 239–243.

Steigemann, W. (1974). Die Entwicklung und Anwendendung von Rechenverfahren und Rechenprogrammen zur Strukturanalyse von Proteinen am Beispiel des Trypsin–Trypsininhibitor Komplexes, des freien Inhibitors und der L-Asparginase. PhD thesis, Technical University of Munich, Federal Republic of Germany.

Symington, L. S., and Kolodner, R. (1985). Partial purification of an enzyme from *Saccharomyces cerevisiae* that cleaves Holliday junctions. Proc. Natl. Acad. Sci. USA *82*, 7247–7251.

Takahagi, M., Iwasaki, H., Nakata, A., and Shinagawa, H. (1991). Molecular analysis of the *Escherichia coli ruvC* gene, which encodes a Holliday junction–specific endonuclease. J. Bacteriol. *173*, 5747–5753.

Takahagi, M., Iwasaki, H., and Shinagawa, H. (1994). Structural requirements of substrate DNA for binding to and cleavage by RuvC, a Holliday junction resolvase. J. Biol. Chem. *269*, 15132–15139.

Tanaka, I., Yao, M., Suzuki, M., Hikichi, K., Matsumoto, T., Kozasa, M., and Katayama, C. (1990). An automatic diffraction data collection system with an imaging plate. J. Appl. Cryst. *23*, 334–339.

Terwilliger, T. C., Kim, S.-H., and Eisenberg, D. (1987). Generalized method of determining heavy-atom positions using the difference Patterson function. Acta. Cryst. (A) *43*, 1–5.

Tsaneva, I. R., Muller, B., and West, S. C. (1992). ATP-dependent branch migration of Holliday junctions promoted by the RuvA and RuvB proteins of E. coli. Cell *69*, 1171–1180.

Tsaneva, I. R., Muller, B., and West, S. C. (1993). RuvA and RuvB proteins of *Escherichia coli* exhibit DNA helicase activity in vitro. Proc. Natl. Acad. Sci. USA *90*, 1315–1319.

von Kitzing, E., Lilley, M. J., and Diekmann, S. (1990). The stereochemistry of a four-way DNA junction: a theoretical study. Nucl. Acids Res. *18*, 2671–2683.

Wang, B. C. (1985). Resolution of phase ambiguity in macromolecular crystallography. Meth. Enzymol. *115*, 90–112.

West, S. C. (1992). Enzymes and molecular mechanisms of genetic recombination. Annu. Rev. Biochem. *61*, 603–640.

West, S. C. (1994). The processing of recombination intermediates: mechanistic insights from studies of bacterial proteins. Cell *76*, 9–15.

West, S. C., and Korner, A. (1985). Cleavage of cruciform DNA structures by an activity from *Saccharomyces cerevisiae*. Proc. Natl. Acad. Sci. USA *82*, 6445–6449.

Wilson, K. S. (1978). The application of *MULTAN* to the analysis of isomorphous derivatives in protein crystallography. Acta Cryst. (B) *34*, 1599–1608.

Yang, W., Hendrickson, W. A., Crouch, R. J., and Satow, Y. (1990). Structure of ribonuclease H phased at 2 Å resolution by MAD analysis of the selenomethionyl protein. Science *249*, 1398–1405.